MINERALOGICAL MAGAZINE, DECEMBER 1981, VOL. 44, PP. 471-83

Uraninite-albite veins from the Mistamisk Valley of the Labrador Trough, Quebec

L. KISH

Ministère de l'Energie et des Ressources, 1620 boul. de l'Entente, Quebec G1S 4N6, Canada

AND

M. CUNEY*

Centre de Recherches sur la Géologe de l'Uranium, B.P. 23, 54500 Vandoeuvre lès Nancy, France

ABSTRACT. The uraninite-albite veins of the Mistamisk area occur in the argillite member of the Dunphy Formation, which is near the base of the slightly metamorphosed Lower Proterozoic sequence of the central Labrador Trough. The vein minerals are albite, uraninite, dolomite, and chlorite, and minor quantities of quartz, tellurides, sulphides, gold, and organic material. Pitchblende and calcite are related to late remobilization.

The veins were deposited in fractures by hydrothermal solutions, and metasomatism caused albitization of wall rocks. Fluid inclusions have an unusual composition, described here for the first time in connection with soda-metasomatism; the aqueous solution of the inclusions is oversaturated in NaCl and contains Ca^{2+} and Mg^{2+}, and the gas phase mostly consists of N_2, CO and CO_2. The presence of hematite and absence of hydrocarbons indicates that the vein-forming solution was oxidizing.

The temperature and pressure of vein formation, estimated from fluid inclusion data, was 300°-350° and 2.5 kbar respectively consistent with the composition of the phengite which is a common metamorphic mineral of the host rock. Vein emplacement occurred in the waning stages of the Hudsonian Orogeny, the hydrothermal solution possibly originating by metamorphism of sodic schists of the Mistamisk area, which are possibly of evaporitic origin.

THE Labrador Trough of eastern New Quebec and Labrador, Newfoundland is a Lower Proterozoic basin, which is known mostly for its sedimentary iron deposits. One of Canada's most important iron mining districts, the Schefferville area occurs in the south. Until recently exploration in the Trough was directed towards economic evaluation of the iron and base-metal occurrences, the latter being less important.

Uranium exploration became important following the discovery of uranium and thorium concentrations in the basal formation of several Proterozoic basins. In the early 1970s syngenetic occurrences were found in the central and northern Trough which are being further explored. A new aspect in uranium exploration was introduced when in 1975 uranium-bearing veins were discovered in the Mistamisk Lake area, central Trough (fig. 1) followed by the discovery in 1976 of boulders of coarse albite and up to 35 % uraninite about 1 km SE of the veins (Kish and Tremblay-Clark, 1978). Later an outcrop of the veins was located by detailed radiometric surveying near to the boulders beneath $\frac{1}{2}$ m of glacial over-burden (Kish and Tremblay-Clark, 1979).

The economic potential of the area is presently being evaluated by exploration companies and preliminary mineralogical, geochemical, and fluid inclusion studies of the Mistamisk uranium occurrences are reported here.

Geological setting

The Labrador Trough is a Proterozoic basin about 800 km long that extends between latitudes 52° 30′ and 59° 00′. The basin is in the Churchill structural Province and is delimited by Archaean gneisses of the Superior Province to the west, by high-grade rocks of the Grenville Province to the south and by a belt of Proterozoic and Archaean gneisses to the east (fig. 1). The geology and stratigraphy in the Trough are summarized by Dimroth (1978). In its early history a central uplift divided the Trough into two sub-basins. The western miogeosynclinal basin is composed mainly of clastic sediments and chemical precipitates, whereas in the eastern eugeosynclinal basin the

---

* And Centre de Recherches Pétrographiques et Géochimiques C.O. no. 1, 54500 Vandoeuvre lès Nancy, France.

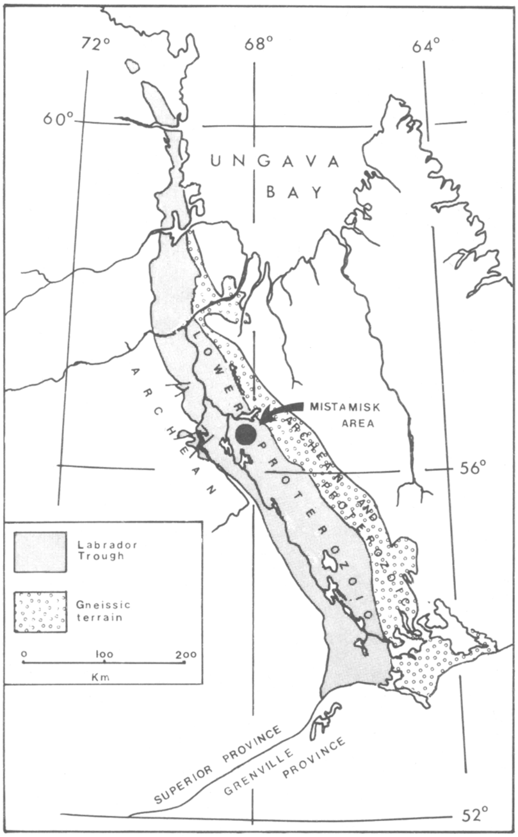

FIG. 1. Geological subdivision of the Labrador Trough.

sequence contains predominantly volcanic and gabbroic rocks.

The last major tectonic event that deformed and metamorphosed the rocks of the Trough and basement to the east was the Hudsonian Orogeny between approximately 1900 and 1600 Ma (Wanless *et al.*, 1968). The basement gneisses west of the Trough were not metamorphosed during this event and yield Kenoran ages (2400–2500 Ma). To the south all sedimentary and basement rocks were completely tectonized, reconstituted and deformed during the Grenville Orogeny (900–1100 Ma).

In the western miogeosynclinal basin the diagnostic metamorphic minerals are albite, phengite, and chlorite. The grade of metamorphism increases eastward and medium-grade (hornblende, staurolite, biotite) assemblages occur in the gneisses of the eastern border zone (Dimroth and Dressler, 1978).

In the central Trough between latitudes 56° 15′ and 56° 30′ a marked divergence from the general NNW structural trend occurs with the development of WSW-oriented cross structures; complex folding and faulting and dykes and diatremes of carbonatite and lamprophyre occur. The Mistamisk Valley, with its rare uraninite–albite veins, is located in this structurally complex area.

The wedge-shaped Mistamisk Valley, transects hills of basalt and gabbro; it is about 3 km wide near Mistamisk Lake, broadening south eastwards. The valley is underlain by fine-grained clastic and chemical sediments (fig. 2). Dimroth (1978) suggested that the basalt–gabbro sequence once formed a continuous cover over the sediments, which were later upthrust against the volcanic rocks along the faults which bound the valley.

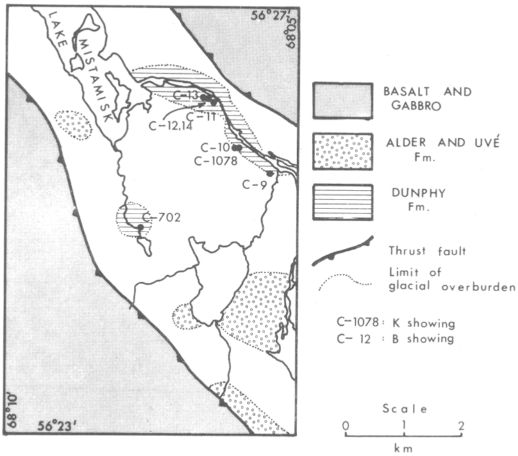

FIG. 2. Geology of the northern Mistamisk Valley and location of the samples (Geology after Dimroth, 1978).

The sedimentary rocks around Mistamisk Lake belong to the Dunphy Formation of the Seward Subgroup (Dimroth, 1978) consisting of interbedded dolomite and fine-grained clastic rocks. South of Mistamisk Lake the dolomite is grey with beige and chocolate weathering; the argillite, siltstone, and slate are creamy coloured, greenish or purple indicating varied oxidation. The absence of coarse clastic and fine laminations of the argillite suggest deposition in a quiet shallow-marine environment. The sedimentary sequence was tightly folded about N–S trending axes overturned to the west. The folds are disrupted by small-scale cross faults.

Mineralogy and chemistry of the rocks

The Mistamisk Valley sediments are slightly recrystallized, but fine sedimentary features such as laminations are well preserved. The argillite and silty rocks are schists or phyllites, composed of an assemblage of quartz, phengite, albite, minor chlorite, and accessory monazite and allanite characteristic of low-grade regional metamorphism. Chemical analyses of selected samples are given in Table I. The average argillite (C-9 and 13, fig. 2) contains 2–3 ppm U, 15–30 ppm Th; K predominates over Na and Mg exceeds Fe.

The dolomite is recrystallized to a fine-grained sugary mass, which is locally interlayered with pelites. The slates contain more Fe than the argillites and have a purplish colour due to hematite dust. In some outcrops slate is bleached

TABLE I. *Chemical analyses of selected rock samples*

%	C-9	C-13	C-702A	C-702B	C-10F	C-10D	C-12A	C-12T	C-14	C-11
SiO_2	59.29	63.25	44.24	53.79	60.73		66.70		61.80	55.23
Al_2O_3	23.78	19.44	13.53	19.52	18.89		18.78		17.16	15.35
Fe_2O_3T	1.71	1.65	2.12	1.69	0.13		0.16		4.90	2.52
MnO	n.d.	n.d.	0.09	0.08	0.04		n.d.		0.06	0.06
MgO	2.36	3.32	8.26	4.09	1.20		0.16		1.31	5.34
CaO	n.d.	n.d.	8.99	4.14	1.39		n.d.		0.78	4.21
Na_2O	4.17	3.15	2.93	6.02	11.10		10.83		9.85	8.43
K_2O	4.65	4.84	3.04	2.55	0.33		0.60		0.35	1.10
TiO_2	0.85	0.73	0.46	0.63	0.03		0.75		0.29	0.60
P_2O_5	n.d.	n.d.	0.18	n.d.			n.d.		n.d.	n.d.
L.I.	3.71	3.17	15.77	7.31			0.42		2.65	7.22
Total	100.52	99.55	99.61	99.82			98.40		99.15	100.06
FeO	0.66	0.37	1.16	0.48			0.11		0.14	0.32
CO_2	0.10	0.11	12.38	5.78			0.18		1.18	6.30
ppm										
V	182	103	73	134	—	n.d.	31	40	14	47
Cr	126	110	69	116	—	—	92	—	14	33
Ni	43	83	57	86	237	310	38	140	<10	51
Cu	43	97	350	47	123	30	58	0.1%	<10	24
Zn	171	25	18	30	35	n.d.	29	n.d.	26	24
Rb	188	178	93	78	i.f.	i.f.	14	n.d.	12	38
Sr	37	34	66	58	77	17	27	231	28	47
Y	12	12	—	36	34	0.32%	7	0.16%	12	26
Zr	150	150	—	89	—	215	113	n.d.	110	156
Mo	3	4	—	—	1	4	2	3	4	3
Ba	772	655	304	321	—	—	76	800	107	57
Pb	1	5	—	14	—	5%	0.14%	1%	33	95
Th	31	16	—	14	n.d.	i.f.	n.d.	i.f.	84	130
U	2	3	9	16	1%	30%	0.08%	6%	270	0.18%

C-9	Creamy coloured thinly laminated argillite
C-13	Pale grey thinly laminated argillite
C-702A	Calcareous green argillite
C-702B	Altered crumbly argillite, locally malachite stained
C-10F	Silicate fraction of a highly radioactive boulder near K2 vein
C-10D	Opaque fraction of the above boulder
C-12A	Metasomatized laminated argillite at the contact of a B vein
C-12T	Radioactive vein material in contact with the above argillite
C-14	Red-stained metasomatized siltstone near B veins
C-11	Red-stained albitized calcareous siltstone adjacent to a B vein

Abbreviations:

L.I.	loss on ignition
n.d.	not detected
i.f.	interference in analysis
Fe_2O_3T	total iron content given as Fe_2O_3.

and ferric iron is reduced along cross-cutting fractures.

Uranium occurrences

Two sets of uraniferous veins are located 1 km E. and 2 km SE of Mistamisk Lake, and are named 'K' and 'B' showings respectively (fig. 2). Most of the chemical and mineralogical characteristics discussed here are for the K showing where the veins are relatively thick, and unaltered material is readily available.

The K showing

Two veins, K2 and K3 were exposed during exploration. Vein K2 has an exposed length of about 15 m, is 25 to 30 cm thick, trends NNW, with an almost vertical dip. Vein K3, 30 m NE of K2, is about 15 cm thick and has the same attitude as K2.

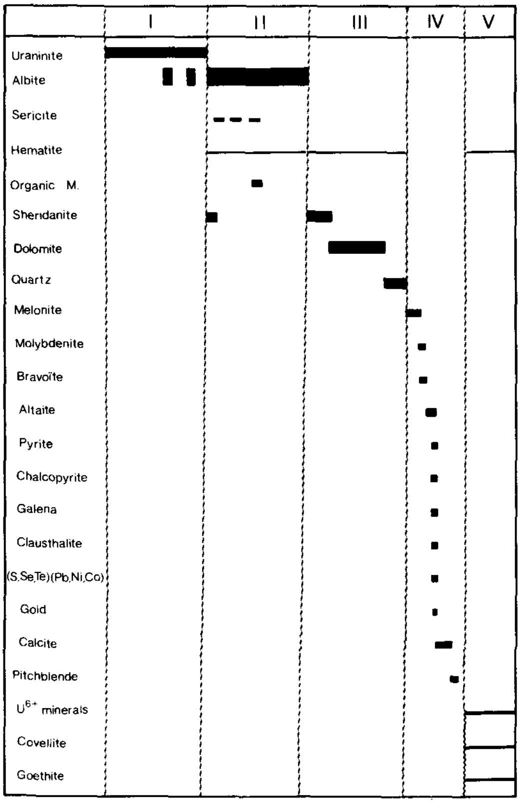

FIG. 3. Paragenesis of the Mistamisk veins.

The main constituents of the K veins in order of abundance are albite, uraninite, dolomite, and chlorite. Quartz, telluride minerals, and alteration products of uranium and iron are minor constituents. The proportion and grain size of the minerals vary over short distances and abundant rock fragments are mixed with vein minerals in some parts of the veins. The mineral paragenesis is presented in fig. 3.

Albite forms crystals up to 3 cm long, oriented randomly except at the margin of the veins where they are perpendicular to the contact (fig. 4.1). The crystals show twin lamellae, displacement along microfractures and brecciation (fig. 4.2) and are pink due to evenly distributed 1–5 μm hematite lamellae and to hematite coating cleavages and microfractures. Fine-grained white mica occurs in the albite, adjacent to the sericite schist wall rock. Carbonaceous inclusions with no birefringence or anisotropy and containing no uranium occur locally as rounded pods, several millimetres long (fig. 4.7).

The formula of albite, calculated from chemical analyses (Table II) is $(Na_{1.011}Ca_{0.004}K_{0.005})Al_{1.004}Si_{2.992}O_8$.

Uranite is unevenly distributed, but is generally concentrated in the axial part of the vein forming masses of closely packed cm-size crystals, some with well-developed cubic faces (fig. 4.4). The uraninite is fractured and recemented by albite and carbonate (fig. 4.3), so that it was among the first minerals to crystallize. Albite is sometimes included in uranite. Yellow alteration products coat uraninite crystals and occur on fractures in uraninite, albite, and carbonate grains.

Unit cell measurements on four uraninite samples from the K2 vein give variable diffraction patterns with a mean a_0 of 5.468 Å, which is close to that of synthetic UO_2 (5.470 Å). A division of the uraninite peaks for some samples (fig. 5) indicates two cubic cells, with a_0 spacings 5.482 Å, and 5.448 Å, the first being dominant. The uraninite contains only traces of thorium and rare-earth elements, but yttrium reaches several thousand ppm (Table I). Determination of U^{4+} and U^{6+} by impulsion polarography (Cathelineau *et al.*, 1979) gives the formulae $UO_{2.318 \pm 0.008}$ and $UO_{2.370 \pm 0.015}$.

Chlorite makes up to 2–3% of the vein material occurring as green to black crystals several millimetres long, generally coating albite combs before carbonate deposition (fig. 4.5). Locally chlorite occurs on the albitized wall rocks or enclosed in albite and carbonates. Analyses of chlorite (Table II) indicate that the mineral is rich in magnesium with a Fe/Mg ratio varying between limits corresponding to:

$$(Mg_{8.78}Al_{2.35}Fe_{0.95})(Si_{5.48}Al_{2.52})O_{20}(OH)_{16}$$

$$(Mg_{7.51}Al_{2.47}Fe_{2.04})(Si_{5.48}Al_{2.52})O_{20}(OH)_{16}.$$

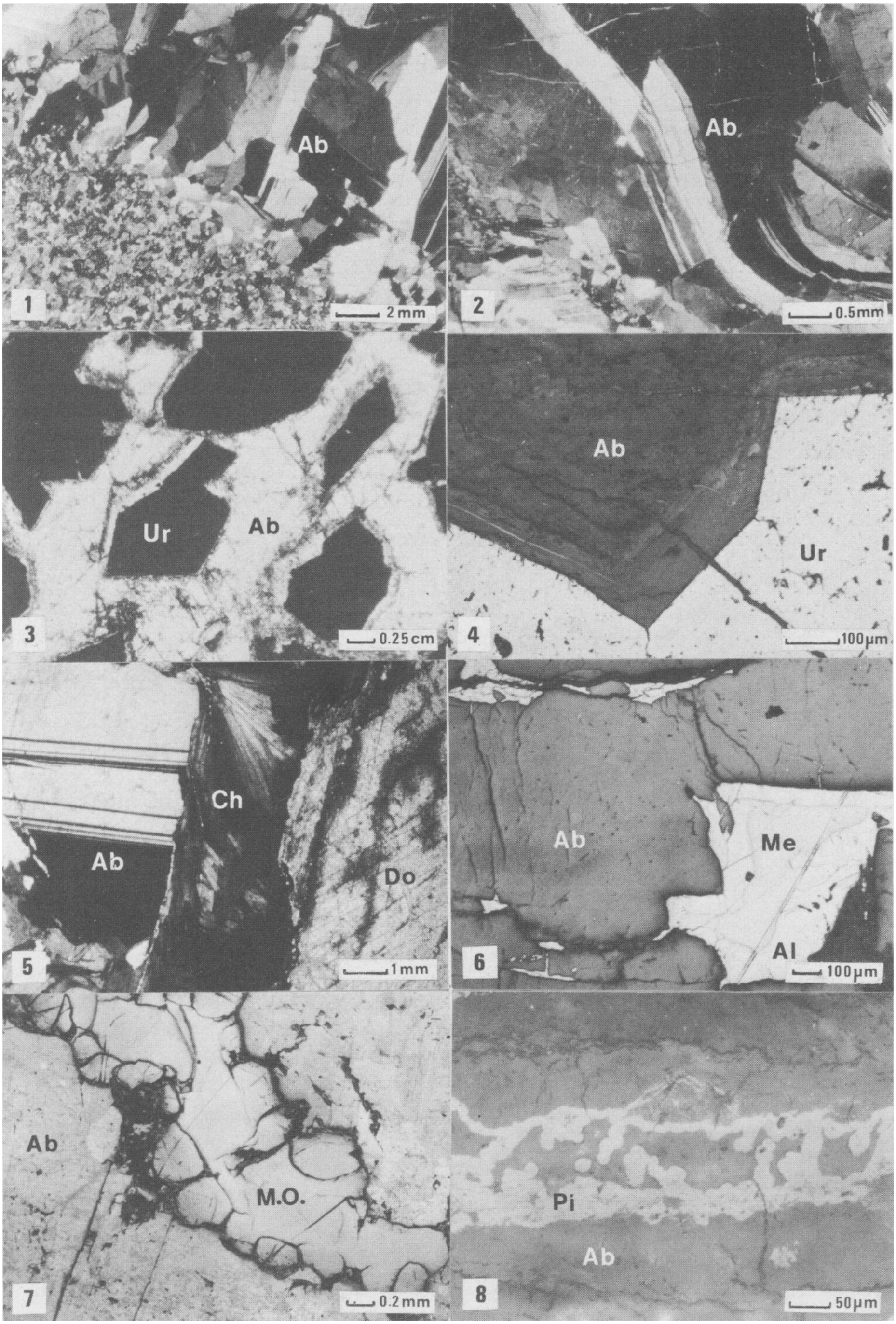

FIG. 4. Photomicrographs showing textural relations in vein samples Ab = albite, Ur = uraninite, Do = dolomite, Ch = chlorite, Me = melonite, Al = altaite, M.O. = organic material, Pi = pitchblende. (1) Contact between albitized argillite and vein, K showing. (2) Vein albite, deformed during growth, K showing. (3) Brecciated uraninite cemented in albite, K showing. (4) Idiomorphic uraninite in albite. (5) Albite-chlorite-dolomite sequence, K showing. (6) Tellurides in fractured albite, K showing. (7) Organic material in albite, B showing. (8) Pitchblende spherules, veinlet in albite, B showing.

TABLE II. *Microprobe analyses of minerals*

	Albite n = 5		Chlorite (1)		Chlorite (2)		Chlorite (3) n = 16		Dolomite (3) n = 5	
Na_2O	11.97		0.00		0.02		0.01		0.01	
K_2O	0.09		0.04		0.01		0.01		0.01	
Al_2O_3	19.56		21.49		22.25		21.38		0.01	
SiO_2	68.59		28.46		27.85		28.51		0.01	
CaO	0.07		0.00		0.03		0.02		28.78	
MgO	0.00		30.40		25.47		28.26		21.60	
FeO	0.00		5.90		12.43		9.07		2.14	
MnO	0.00		0.00		0.06		0.02		0.20	
TiO_2	0.02		0.00		0.02		0.02		0.01	
CO_2 (4)	—		—		—		—		47.23	
	100.29		86.28		88.14		87.30		100.00	
	Si 11.966	15.98	Si 5.48	8.00	Si 5.48	8.00	Si 5.51	8.00	Ca 0.952	2.01
	Al 4.015		Al 2.52		Al 2.52		Al 2.49		Mg 1.000	
	Na 4.042	4.08	Al 2.35	12.08	Al 2.47	12.02	Al 2.38	12.04	Fe 0.055	
	K 0.021		Ti 0.00		Ti 0.00		Ti 0.00		Mn 0.005	
	Ca 0.014		Fe 0.95		Fe 2.04		Fe 1.46			
	Mg 0.000		Mn 0.00		Mn 0.00		Mn 0.00		C 1.99	
	Fe 0.000		Mg 8.78		Mg 7.51		Mg 8.20			
	Mn 0.000		Ca 0.00		Ca 0.00		Ca 0.00			
	Ti 0.000		Na 0.00		Na 0.00		Na 0.00			
			K 0.00		K 0.00		K 0.00			

Explanation:

n	number of spot analyses
(1) and (2)	maximum and minimum Mg/Fe ratios
(3)	average of n analyses
(4)	CO_2 obtained by subtracting the sum of the partial analysis from 100%.

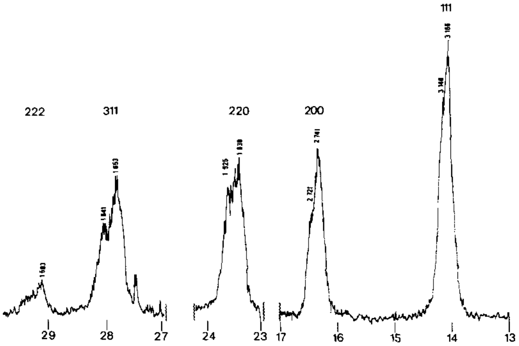

FIG. 5. X-ray diffractogram of uraninite showing double peak diffraction pattern.

The composition corresponds to sheridanite according to Hey (1954), with:

$$0.10 < \frac{Fe_{total}}{Fe_{total}+Mg} < 0.21.$$

Dolomite constitutes about 10% of the vein material. It is coarsely crystalline, either filling voids between albite and uraninite crystals or fractures. The crystals are twinned, containing tiny crystals of hematite. Microprobe analyses of dolomite (Table II) indicate that the iron content is positively correlated with manganese.

Quartz occurs in the non-radioactive part of the K vein filling spaces between large albite laths: its relationship to uraninite is uncertain. Exceptionally it occurs in healed hair fractures in the radioactive part of the vein.

Melonite ($NiTe_2$) forms anhedral blebs or fills fractures in uraninite and albite or hairline cracks in the host rock (fig. 4.6).

Altaite (PbTe) occurs rimming melonite and rarely as independent grains.

Sulphides are rare and are usually associated with altaite—mostly small grains of *chalcopyrite, pyrite*, and *galena*. Chalcopyrite is partly altered to covelline. A sulphotelluride of cobalt containing traces of nickel has been identified by microprobe as inclusions a few microns in diameter in altaite.

Native gold is present in tiny grains (300 to 400 μm) mostly in altaite and melonite (fig. 6).

Goethite occurs as a fracture coating associated

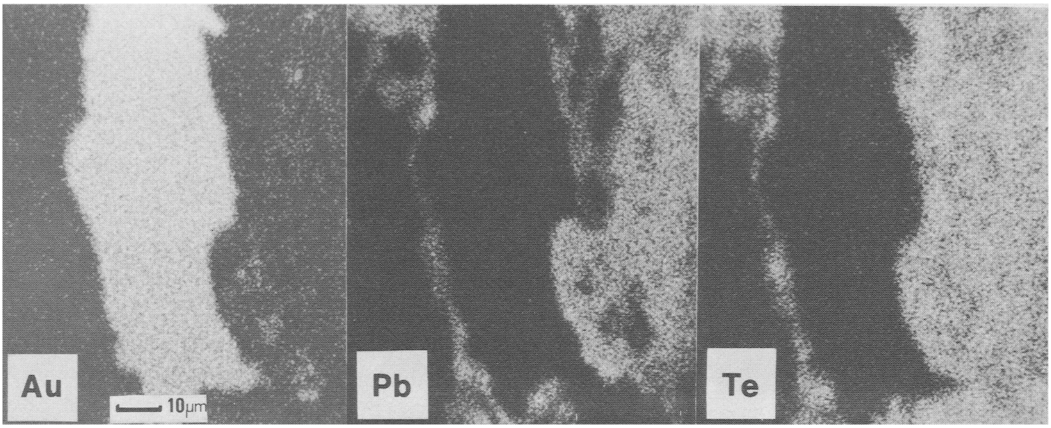

FIG. 6. Electron microprobe image of gold at the margin of altaite.

with hexavalent uranium minerals and is an alteration product.

Calcite occurs as a late trace constituent.

Rock fragments. Angular inclusions of argillite and siltstone up to 3 cm across are abundant in the uranium-rich part of the K2 vein. In other veins host-rock inclusions are scarce. Some fragments are recemented by pink albite. Microscopic examination reveals that the inclusions are composed 0.05–0.1 mm mosaic albite whose Na content is significantly higher than that in the host-rock argillite away from the veins (Table III and fig. 7).

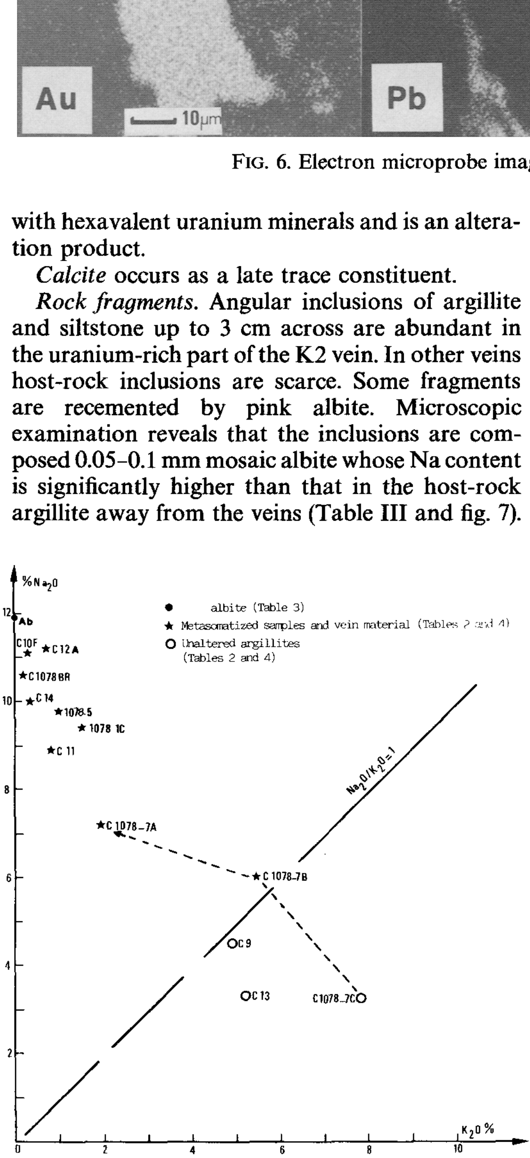

FIG. 7. Plot of K_2O contents against Na_2O contents showing progressive albitization of the wall rock.

The mineralogy of the B veins is similar to that of the K veins, but the proportion of the minerals is different and they are more altered, for example some uraninite crystals are completely altered to greenish yellow secondary minerals showing weak radioactivity.

The radioactive boulders that led to the discovery of the K showing have the same mineralogy and textures as the K veins.

Wall-rock-vein contact

Along the contact with the veins, the host rock is altered in a zone a few centimetres wide. The main mineralogical change is the development of albite at the expense of sericite. The effect of the sodic vein-forming solution was to increase the Na/K ratio in the wall rock at the contact and in the rock fragment inclusions compared with unaltered host rock (fig. 7).

Fluid inclusions

Fluid inclusions were investigated with a Chaix Meca microthermometry apparatus (Poty *et al.*, 1976). Temperatures were corrected using a calibration curve derived from the melting temperatures of chemical standards.

Fluid inclusion types

Fluid inclusions are numerous and evenly distributed in albite, dolomite and quartz of the K and B veins. They are commonly up to 8 µm in diameter, although in one quartz sample of the B showing especially large examples (10–60 µm) were found. The inclusions are filled with an aqueous solution, a gas bubble which constitutes 2–5% of the volume, and several solid phases (fig. 8). These are: halite cubes, forming generally 5–10% of the inclusion

TABLE III. *Na_2O and K_2O contents (%) of contact specimens and inclusions, K2 vein*

	Na_2O	K_2O	
C-1078-5	9.80	1.00	Angular inclusion of argillite
C-1078-IC	9.44	1.52	
C-1078-BR	10.60	0.18	Albitized silty argillite in contact with the vein
			Samples across 5 cm contact zone
C-1078-7A	7.20	1.88	7A Pinkish albitized argillite, contact specimen
C-1078-7B	6.00	5.40	7B Partly metasomatized argillite–sericite schist
C-1078-7C	3.30	7.80	7C Pale-green laminated argillite–sericite schist

volume, but may reach 40% in some; small anisotropic globulous or rhombohedral grains, possibly a carbonate, in 10–20% of the inclusions making up to 1% of the volume; automorphic hematite forming tiny lamellae mostly in the inclusions in albite and dolomite, rarely in quartz.

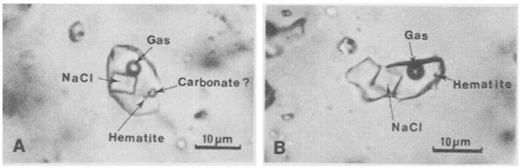

FIG. 8. Fluid inclusions in quartz crystals, K showing.

For microthermometric determinations, only fluid inclusions in quartz were used. The pressure resistance of albite and dolomite is relatively small and, on heating, inclusions decrepitate at about 200 °C, before any phase transition.

Raman microprobe data

Components identified in the gas phase by Raman microprobe (Dhamelincourt *et al.*, 1979) are N_2, CO_2, CO, and H_2. Hydrocarbons, H_2O and O_2 were not found. The component SO_2 cannot be identified in quartz host crystals because of the overlap of the emission lines of SO_2 and quartz. For a typical fluid inclusion in quartz the calculated proportions of components in mole % with an estimated maximum relative error of 20%, are as follows:

$$N_2 = 73.0\%,\ CO_2 = 16.8\%,\quad CO = 9.9\%,\ H_2 = 0.3\%.$$

Freezing data

Solidification of the aqueous solution occurs at −90 °C. The ice begins to melt at −60 °C, i.e. slightly lower than the eutectic minimum of the experimental system $NaCl\text{-}CaCl_2\text{-}MgCl_2\text{-}H_2O$ which is −57 °C (Luzhnaya and Vereshtchetina, 1946). The measured range of the final melting temperature of the ice in the Mistamisk inclusions is −38.2 to −35.2 °C. The close resemblance of the measured temperatures to the experimental data of the system mentioned above suggests the presence of cations such as Ca^{2+} and Mg^{2+}, in addition to Na^+ and K^+, in the Mistamisk solutions.

A hydrate with refractive index lower than that of ice was noted after the melting of the ice. This hydrate is highly metastable; it does not appear systematically in all inclusions and may crystallize only during repeated runs. Its formation was never observed on cooling before the crystallization of the ice.

The final melting temperature of the hydrate is between 0 °C and ±1.4 °C. Slow cooling of the inclusion just before the final melting of this hydrate leads to the formation of hexagonal hydrate crystals with simultaneous resorption of the halite cubes. The dissolution of the halite is rarely complete because generally the hydrate forms a barrier between the halite crystals and the aqueous solution and stops further growth. Hydrohalite is known to form under similar conditions, and so the hydrate of the Mistamisk fluid may be a hydrohalite, although its melting temperature does not correspond to the data of the experimental system mentioned above.

Another hydrate with a still lower refractive index occurs as tiny needles, and melts between +13 and +15 °C. The gas phases of the inclusions may be involved in the formation of this hydrate, but the lack of relevant experimental data, especially on the formation of CO hydrate, prevents identification of this second hydrate.

No phase transformation was observed in the gas phase; thus its density cannot be estimated. As the gas bubble generally does not exceed 3 μm in diameter, up to 40% of its volume can be a liquid without being microscopically observable, owing to limitations in optical resolution. This also prevents the calculation of the bulk composition of the inclusions.

Heating data

Inclusions in quartz larger than 10 μm decrepitate at about 250 °C before any phase transformation occurs. In smaller inclusions some homogenization temperatures are below 150 °C but appear to be related to 'necking-down'. Some inclusions homogenize above 200 °C, but after cooling the gas bubble occupies a larger volume in the inclusion than before heating, suggesting that leakage occurred. Reproducible, reliable homogenization temperatures fall between 160 and 180 °C. Halite crystals are dissolved generally between 300 and 350 °C in the inclusions that do not decrepitate. The carbonate and hematite are still not dissolved at 350 °C.

Uranium-lead ages

Ages determined on one sample from the K vein, one from the mineralized boulder and one from the B vein are presented in Table IV and plotted on a concordia diagram in fig. 9. They are discordant and show variable Pb loss, the smallest loss being for uraninite from the K veins. The largest lead loss was for the B veins where pitchblende has been observed. The upper intercept of concordia gives an age of *c.*1800 Ma for uraninite deposition which corresponds to the Hudsonian orogeny. The lower intercept gives an age of *c.*400 Ma for the remobilization of uranium as pitchblende.

Interpretations

The unusual element associations, the composition of the fluid inclusions and the textural and contact relations of the uraninite-albite veins reflect the chemistry of the hydrothermal solutions

TABLE IV. *Analytical results obtained on three mineralized samples*

		U%	Pb% total	Pb% Common	$^{207}Pb/^{235}U$	Age (Ma)	$^{206}Pb/^{238}U$	Age (Ma)
1	K Vein	62.18	14.47	0.0029	3.477	1522	0.2454	1415
2	Boulder	67.841	10.467	0.000911	2.184	1175	0.1636	977
3	B Vein	43.432	3.125	0.02594	0.6754	524	0.0786	488

The analyses were made by private laboratories (1) Geospec (Canada), (2) and (3) Teledyne (USA).

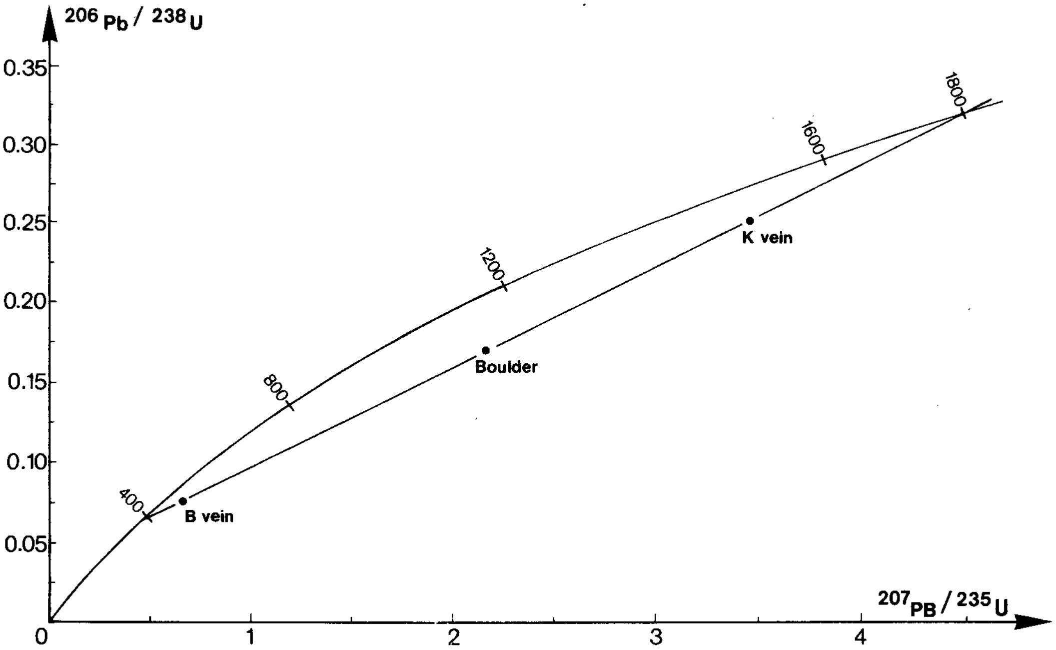

FIG. 9. Concordia diagram. Discordant ages of the Mistamisk samples.

and the pressure-temperature conditions of vein emplacement.

Chemical characteristics of the vein-forming fluid

The composition of fluid inclusions in early albite is similar to that of late dolomite and quartz so that the fluid composition did not change significantly during crystallization of the minerals, although minor variations probably explain the crystallization of different assemblages. All of the ionic species (Na^+, Ca^{2+}, Mg^{2+}, Fe^{3+}, CO_2) of the main silicate minerals except Al^{3+}, which has low solubility in aqueous solutions, are found in the fluid inclusions. Dawsonite ($NaAl_2(CO_3)_2 \cdot 2H_2O$) has been observed in fluid inclusions elsewhere (Coveney and Kelly, 1971; Roedder, 1972), suggesting that alumina is transported in solutions containing sodium and CO_2.

The marked increase in Na/K ratios in the wall rock corresponding to the replacement of potassic mica by albite reflects the Na^+ activity of the hydrothermal solutions. The likely reaction can be written as follows:

$$KAl_3Si_3O_{10}(OH)_2 + 6SiO_2 + 3Na^+ \rightleftharpoons 3NaAlSi_3O_8 + K^+ + 2H^+ \quad (1)$$

The formation of three moles of albite from one of potassic mica approximately doubles the total molar volume. The transformation did not, however, cause a volume change in the wall rock because sedimentary laminations in the metasomatized argillite are preserved. The albite was therefore confined to opening fractures, developing in columnar habit perpendicular to the contact. Reaction (1) also leads to an increase in HCl activity, i.e. in H^+ activity because HCl is almost completely dissociated below 300 °C (Helgeson, 1969). This, and the high NaCl content of the solution, increase the solubility of the Ca, Mg, and Fe carbonates (Holland and Malinin, 1979), so that crystallization of carbonates follows albitization consistent with the interstitial position of the carbonate in the K veins.

The growth of chlorite instead of albite is controlled by the equilibrium:

$$4.5NaAlSi_3O_8 + 8Mg^{2+} + 1.5Fe^{2+} + 0.5Fe^{3+} + 16H_2O \rightleftharpoons Mg_8Fe_2Al_{4.5}Si_{5.5}O_{20}(OH)_{16} + 4.5Na^+ + 8SiO_2 + 16H^+ \quad (2).$$

Thus the increase in activity of Mg^{2+}, Fe^{2+} and the decrease in activity of Na^+ and SiO_2 caused by reaction (1) favours chlorite stability whereas the increase in activity of H^+ has a reverse effect.

Albitization requires six moles of silica per mole of potassic mica which prevents early crystallization of quartz, whereas the growth of chlorite has the reverse effect. With increasing sodium content potassium is depleted, and in contact specimens potassium appears to have been almost completely leached. Other changes related to soda metasomatism are an increase in the iron content and a decrease in barium and rubidium contents. (Table I). Hence slight changes in the activity of dissolved ionic species cause gangue minerals to crystallize in variable proportions from the same solution in different parts of the vein.

The composition of the associated gas phase is an important control on redox conditions, which together with complexation are the principal controls in uranium deposition (Nguyen Trung, 1980). Analysis of the gas phase of the Mistamisk fluid inclusions, identifies CO_2, CO and H_2 without hydrocarbons or other reduced species, suggesting oxidizing conditions during quartz deposition (if the gases remained in thermodynamic equilibrium since entrapment). This is confirmed by the presence of hematite in fluid inclusions and vein minerals. N_2 is overwhelmingly abundant in the gas phase. The presence of nitrogen in fluid inclusions has been known for several years (Roedder, 1972), and it has been found recently in large amounts in such different geological environments as the very low-grade evaporitic association of northern Tunisia (Guilhaumou *et al.*, 1978), black shales of the Alps (Dhamelincourt *et al.*, 1979) and granulite-facies gneisses of SW Norway (Swannenberg, 1980). In the slightly metamorphosed part of the shale sequence of the Alps, nitrogen is associated with reduced species such as methane and higher hydrocarbons, and may be related to decomposition of organic matter in the black shales. Inclusions in the evaporites of northern Tunisia are of particular interest because they are of similar composition to the Mistamisk inclusions: they are saturated in NaCl, their N_2/CO_2 ratios are up to 9.3 and methane is absent. In the Tunisian evaporites, the NaCl originates from the dissolution of halite, the CO_2 is related to decarbonation reactions, and the nitrogen is from the decomposition of organic material. Some of the carbonaceous material in the early albite of the Mistamisk veins is interpreted as immiscible heavy hydrocarbon drops in suspension, which may not be in equilibrium with the solution.

The more oxidizing conditions of the veins of Mistamisk and North Tunisia relative to the Alps reflect defluidization of more oxidized lithological facies during progressive metamorphism.

Pressure and temperature evaluation

Accurate *P–T* determinations from the microthermometric measurements is difficult because of an early decrepitation of the fluid inclusions and the complexity in the composition of the mixtures involved. The interval found for the homogenization temperature (160–180 °C) is the minimal estimate of the trapping temperature. NaCl crystals are dissolved between 300 and 350 °C in the inclusions that did not decrepitate. In the pure H_2O-NaCl system these temperatures correspond to NaCl equivalents of 38–42 wt. % (Keevil, 1942). Considering the presence of the other ions and gases in the Mistamisk inclusions this percentage is an overestimate of the real NaCl concentration. Some large halite crystals fill up to 40% of the inclusion volume, suggesting oversaturation at the time of entrapment and in this case the temperature of 300 to 350 °C may represent the real trapping temperature (Touray, 1970). The available *P–V–T* data are limited to 25% NaCl solution (Hilbert, 1979). For a mean homogenization temperature of 180 °C and 25% NaCl the isochore indicates a density of 1.075 g cm^{-3}. Higher salt contents increase the slope of the isochores at a given temperature, whereas the presence of gases like CO_2 and N_2 has the opposite effect. If we assume that in the case of the Mistamisk fluids these two opposing effects cancel each other, then for a trapping temperature of 325 °C the pressure corresponding to the 1.075 g cm^{-3} isochore is 2.5 kbar. Because of the lack of experimental data this *P–T* evaluation provides only a general indication and precludes the estimation of error limits.

TABLE V. *Chemical analyses of the phengites of the enclosing argillite (TFC 13c)*

	Phengite n = 10	
Na_2O	0.23	
K_2O	10.52	
Al_2O_3	30.70	
SiO_2	48.47	
CaO	0.01	
MgO	2.45	
FeO	1.46	
MnO	0.04	
TiO_2	0.21	
Total	94.09	
Si	6.532	8.00
Al^{IV}	1.468	
Na	0.060	1.87
K	1.809	
Ca	0.002	
Al^{VI}	3.410	4.08
Mg	0.492	
Fe	0.164	
Mn	0.005	
Ti	0.011	
(1) $\frac{Na}{Na+K} \times 100$	3.2	
(2) $\frac{Si-6}{2} \times 100$	26.6	

(1) Paragonite substitution
(2) Celadonitic substitution
n = number of analyses.

Idiomorphic uranium dioxide crystals are generally regarded as indicating high temperature (Rich *et al.*, 1977), although it has been synthesized at 25 °C (Kochenov *et al.*, 1977) indicating that other factors besides the temperature, affect the crystallization of the uraninite.

The flame texture of albite in the K showing is similar to that of the early quartz crystals which grew during the opening of fissures contemporaneous with low-grade alpine metamorphism.

The *P–T* conditions of the regional metamorphism can be estimated from the composition of the white mica of the metamorphosed argillite host rock (Table V). The silica content of this mica, a phengite, is plotted on Velde's (1965) experimental diagram in fig. 10. For a temperature of 300 to 350 °C the estimated pressure of 2.5 to 2.7 kbar is similar to that deduced from microthermometry of the vein minerals.

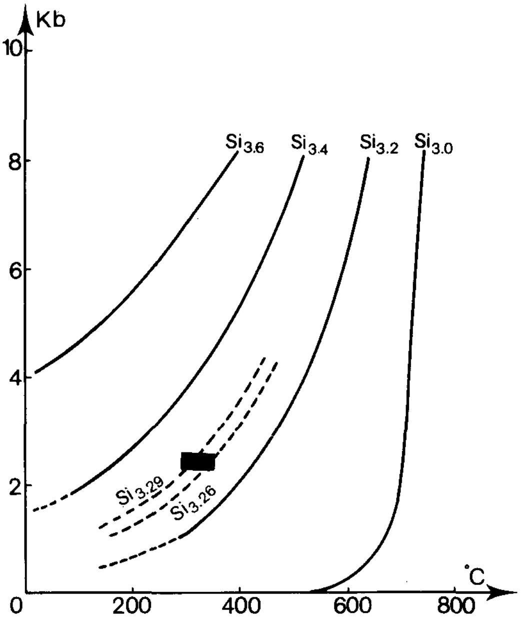

FIG. 10. Silicium charge of phengites of the argillites, plotted on Velde's (1965) experimental diagram. The black square represents *P–T* conditions of vein emplacement obtained from the fluid inclusion data.

Uranium geochemistry

The principal characteristics of the solution from which the uraninite–albite veins were formed are a highly sodic composition and oxidizing conditions. Oxygen fugacity and complexation are the main factors controlling uranium solubility in hydrothermal solutions (Legret, 1979; Nguyen Trung, 1980). The oxidizing character of the Mistamisk fluids and the availability of CO_2 to form uranyl–carbonate complexes led to the transportation of uranium to the site of precipitation.

The deposition of uraninite was probably controlled by changes in the composition of the gas phase which buffers the oxygen fugacity of the fluid. Uraninite was the first mineral to crystallize in the Mistamisk veins so that the evolution of the gas phase before this cannot be studied although the occurrence of hydrocarbons in albite suggests more reducing conditions. The occurrence of pitchblende in the veins corresponds to remobilization probably at a lower temperature and the two cubic cells of uraninite may reflect this. Two cell dimensions were also observed in the uranium oxide from the Cluff Lake deposit (Cathelineau *et al.*, 1979). In those samples automorphic uraninite crystals occur on pitchblende spherules, which is interpreted as a higher temperature remobilized form of pitchblende (Pagel and Ruhlman, 1979). In the Mistamisk veins the X-ray phenomenon is the same, but the pitchblende is secondary after uraninite; that is, the sequence is inverse. The most important X-ray line corresponds to the larger cell of the least oxidized bulk uraninite, which contains yttrium and lead substituting for uranium, whereas the smaller cell reflects an incomplete re-equilibration during the period of a low temperature partial remobilization which locally formed the pitchblende.

Conclusions

The uraninite–albite veins of the Mistamisk area were deposited in the fractured argillites of the Dunphy Formation from a migrating hydrothermal solution. The *P–T* conditions of emplacement, estimated from the microthermometric measurements of the fluid inclusions in vein quartz, are 300–350 °C and 2.5 kbar and the composition of phengite in the host rock argillite indicates similar *P–T* conditions during metamorphic recrystallization. These observations, combined with brecciation and rock fragments in the veins and the U/Pb ages, suggest that emplacement of the veins occurred towards the end of the last major tectonic event (Hudsonian) in the central Trough.

Four stages in the paragenetic sequence of the Mistamisk veins can be distinguished. During the first stage of emplacement tectonically active conditions are indicated by the flame texture of the albite, the brecciated texture of the uraninite, and the angular rock fragments in the veins. During the second stage stable conditions prevailed, with the crystallization of chlorite, dolomite, and quartz. The third stage was a partial remobilization at a lower temperature, demonstrated by the double cell dimension in the uraninite crystal structure and the local occurrence of pitchblende veinlets. The telluride minerals, gold, chalcopyrite, and the tiny grains of accessory sulphide appeared in this stage. Lastly a late-stage alteration produced yellow hexavalent uranium compounds, goethite and iron hydroxides.

An unusual elemental association Na–Mg–U–Y–Te–Ni–Pb–Cu–Au characterizes the Mistamisk veins. The composition of the fluid inclusions is also unusual in containing abundant NaCl, N_2, and CO_2. This composition, described probably for the first time in this paper in connection with soda-metasomatism, is known elsewhere only from rocks of evaporitic origin. The Dunphy dolomite and argillite in the immediate vicinity of the veins are shallow marine sediments. They contain only traces of radioelements, and the content of potassium predominates over sodium. Sodic albite–sericite schists with up to 300 ppm of thorium outcrop in the Mistamisk area, about 8 km ESE of the veins and adjacent to the fault contact of the valley. These radioactive schists, some with finely dispersed pyrite, may have formed a restricted evaporitic sequence from which solutions were expelled during the waning stages of regional metamorphism of the Trough.

Acknowledgements. This work was carried out with collaboration between the Ministère de l'Energie et des Ressources, Quebec; Centre de Recherches Pétrographiques et Géochimiques, Nancy; and Centre de Recherches sur la Géologie de l'Uranium, Nancy. The authors thank B. Poty and T. Clark for critically reading the manuscript and J. Dubessy for Raman microprobe analyses. The work is published with the permission of the 'Ministère de l'Energie et des Ressources' du Québec.

REFERENCES

Cathelineau, M., Cuney, M., Leroy, J., Lhote, F., Nguyen, T. C., Pagel, M., and Poty, B. (1979). Proc. symp. on uranium vein deposits, Lisbonne, to be published.

Coveney, R. M. and Kelly, W. C. (1971). *Contrib. Mineral. Petrol.* **32**, 334–42.

Dhamelincourt, P., Beny, J. M., Dubessy, J., and Poty, B. (1979). *Bull. Mineral.* **102**, 600–10.

Dimroth, E. (1978). Labrador Trough Area. Ministère des Richesses Naturelles du Québec. Geol. Report 193.

—— and Dressler, B. (1978). In *Metamorphism in the Canadian Shield.* Geol. Surv. Can. Paper 78-10.

Guilhaumou, N., Dhamelincourt, P., Touray, J. C., and Barbillat, J. (1978). *C.R. Acad. Sci. Paris*, **287**, 317-19.

Helgeson, H. C. (1969). *Am. J. Sci.* **267**, 729-804.

Hey, M. H. (1954). *Mineral. Mag.* **30**, 277-92.

Hilbert, R. (1979). Chemicingenium Band 2, Hochschulverlag, Freiburg, 212 pp.

Holland, H. D. and Malinin, S. D. (1979). In *Geochemistry of Hydrothermal ore deposits*, 2nd ed., H. L. Barnes (ed.), New York, 461-508.

Keevil, N. B. (1942). *J. Am. Chem. Soc.* **64**, 841-50.

Kish, L. and Tremblay-Clark, P. (1978). *Rapport préliminaire des travaux de 1976*. Ministère des Richesses Naturelles du Québec, Québec. D.P. V-567.

——— (1979). *Rapport préliminaire des travaux de 1977 et 1978*. Ministère des Richesses Naturelles du Québec, Québec. D.P. V-666.

Kochenov, A. V., Korolev, K. G., Dubinchuk, V. T., and Medvedev, Yu. L. (1977). *Geochem. Int.* No. 14, 82-7.

Legret, M. (1979). Unpublished thesis CRPG-ENSG, Nancy, France.

Luzhnaya, N. P. and Vereshtchetina, I. P. (1946). *Zh. Pr. Khim.* **19**, 723-33.

Nguyen Trung, C. (1980). XXVIe Congrès Géologique International, Paris, to be published.

Pagel, M. and Ruhlman, F. (1979). *Bull. Mineral.* **102**, 654-64.

Poty, B., Leroy, J., and Jachimovicz, L. (1976). *Bull. Soc. fr. Mineral. Cristallogr.* **89**, 182-6.

Rich, R. A., Holland, H. D., and Petersen, U. (1977). *Hydrothermal uranium deposits*, Elsevier, New York, 264 pp.

Roedder, E. (1972). In *Data of Geochemistry*, U.S.G.S. Prof. pap. 440-JJ, 164 pp.

Swannenberg, H. E. C. (1980). Ph.D. thesis, Ryksuniversität, Utrecht, 147 pp.

Touray, J. C. (1970). *Schweiz. Mineral. Petrogr. Mitt.* **50**, 67-79.

Velde, B. (1965). *Am. J. Sci.* **262**, 886-913.

Wanless, R. K., Stevens, R. D., Lachance, G. R., and Edmonds, C. M. (1968). *Age determinations and geological studies, K-Ar isotopic ages*. Report 8; Geol. Surv. Can., Paper 67-2, pt. A.

[*Revised manuscript received 11 August 1981*]